Application of ^{29}Si Homonuclear and ^{1}H−^{29}Si Heteronuclear NMR Correlation to Structural Studies of Calcium Silicate Hydrates

F. Brunet,*,† Ph. Bertani,†,§ Th. Charpentier,† A. Nonat,‡ and J. Virlet†

Service de Chimie Moléculaire, URA 331 CNRS, Direction des Sciences de la Matière, CE Saclay 91191 Gif sur Yvette Cedex, France, and Laboratoire de Recherche sur la Réactivité des Solides, UMR 5613 CNRS Université de Bourgogne, 21078 Dijon, France

Received: October 20, 2003; In Final Form: June 21, 2004

Structural characterization of calcium silicate hydrate (C-S-H) is of major importance, as it is the main constituent of Portland cement and is responsible for its principal cohesion and durability properties. In this paper we apply homonuclear and heteronuclear solid-state NMR methods for the investigation of C-S-H. We use double quantum homonuclear ^{29}Si−^{29}Si correlation using the BAck to BAck recoupling scheme to gain information about connectivity between silicates and 2D ^{1}H−^{29}Si HETeronuclear chemical shift CORelation (HETCOR) to characterize the proton environment of the silicate chains. Our observations are in agreement with the tobermorite model and with previous results, but we get evidence of a continuous decrease of the silicate chain length with increasing Ca/Si ratio rather than a bimodal distribution of chain length.

Introduction

Among the most common systems in studies of hydrate concrete is the $CaO-SiO_2-H_2O$ system whose constituents are calcium silicate hydrate (C-S-H) and portlandite ($Ca(OH)_2$). Calcium silicate hydrate (C-S-H) is the main component of Portland cement hydrated paste and is responsible for its principal properties of cohesion and durability.[1] Despite numerous studies[2−7] of the $CaO-SiO_2-H_2O$ system, it is not still satisfactorily described. Indeed the stoichiometry of C-S-H, i.e., the Ca/Si ratio, varies with the calcium hydroxide concentration in the equilibrium solution, and this ratio may vary between 0.6 and 2 for prepared C-S-H while in a neat Portland cement paste it is fixed at 1.7. Most of C-S-H are nanocrystalline porous materials and are thereby difficult to characterize by X-ray diffraction techniques.[5] Recent investigations by atomic force microscopy[8] have shown that the size of aggregated particles is about 50 nm in diameter and 5 nm in thickness. Experimental techniques such as infrared[5,9−10] and Raman spectroscopy[11] and EXAFS[12] and XANES[13] absorption spectroscopy have clearly shown that C-S-H prepared by precipitation from calcium and silicate salts or from silica and lime mixes are composed of layers whose structure is generally similar to that of tobermorite,[14] a natural mineral analogue (Figure 1). Each layer is constituted by a calcium plane intercalated between linear chains of silicates parallel to the calcium planes. In tobermorite the silicate chains are infinitely long and the Ca/Si ratio is about 0.7. These chains of silicate tetrahedral consist of a three-unit repetition pattern ("dreierketten"), i.e., in each group of three tetrahedra, two share their oxygen atoms with the calcium plane ("nonbridging tetrahedra"), and the third ("bridging tetrahedron") does not and has two unshared oxygen atoms bearing a proton (silanol groups). The interlayer contains water molecules and few calcium ions.

The 1.1 nm tobermorite structure, as described by Hamid,[14] is generally used as a model for the structure of C-S-H, particularly at low Ca/Si ratios. However, this structural model is not consistent with the description of prepared C-S-H in which various defects may occur compared to the ideal structure (Figure 1). Indeed at the lowest Ca/Si ratios, interconnection between chains of the same or different layers may occur, whereas at higher Ca/Si ratios, defects such as the shortening of the chains by departure of bridging tetrahedra and partial substitution of silanol protons by calcium ions occurs. It appears that at high Ca/Si ratios (corresponding to the real situation in cement pastes) the structural model remains inadequate needing further investigations to describe the structure of C-S-H which is still controversial.[12,15] Indeed, the limit stoichiometry if all the bridging tetrahedra are missing and all the silanol protons are replaced by calcium ions only corresponds to a Ca/Si = 1.25 Since some silanol protons are always present in C-S-H of high Ca/Si ratio,[12,15] there must exist calcium ions charge-balanced by hydroxide ions which have been already identified.[16] To account for this point, Taylor suggested first[6] that the C-S-H of higher Ca/Si ratios should be structurally close to jennite $Ca_8H_4Si_6O_{18}(OH)_8 6H_2O$ (Ca/Si = 1.33). In that case, only one oxygen site of the nonbridging tetrahedra coordinates the calcium ions of the plane; the other oxygen is provided by hydroxide ions.[17] The C-S-H whose Ca/Si ratios are intermediate should be a mix of both phases in which the tobermorite-like and jennite-like regions could be poorly defined and could merge into each other within individual layers.[18] However, it has been proved from homonuclear correlation NMR experiments that silicon sites of C-S-H samples belong to the same solid phase.[16] Cong and Kirkpatrick,[7] based on their extensive study of synthetic C-S-H of variable Ca/Si ratio using ^{29}Si and ^{17}O MAS and CPMAS NMR, proposed a defect tobermorite-like model for C-S-H in which some silicate portions of the structure derive from tobermorite with missing bridging tetrahedra, others from

* Corresponding author. E-mail: fbrunet@cea.fr. Phone: 33 01 69 08 86 20. Fax: 33 01 69 08 98 06.
† Service de Chimie Moléculaire, URA 331 CNRS.
‡ UMR 5613 CNRS Université de Bourgogne.
§ Present address: Université Louis Pasteur, Institut Lebel, 67000 Strasbourg, France.

10.1021/jp031174g CCC: $27.50
Published on Web 09/11/2004

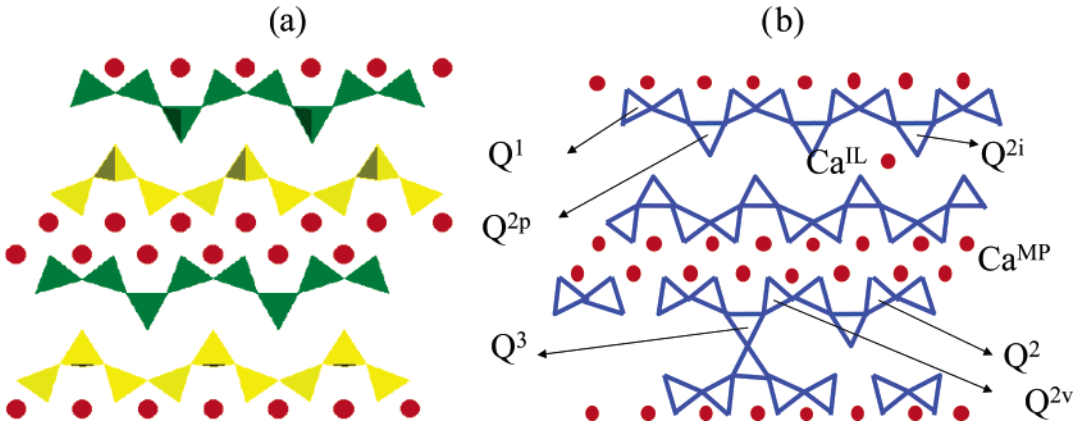

Figure 1. (a) The layered structure of tobermorite is composed of a calcium plane (red dots) bordered by two silicate planes (yellow and green chains) and separated by the interlayer space containing water molecules, hydroxyl groups and some calcium ions. (b) The silicate planes are composed of silicate chains with a specific three-unit repetition ("dreierketten"): two silicate tetrahedra, noted as Q^2, are coordinated by calcium planes (red dots) whereas the third silicate (called the bridging tetrahedron and noted as Q^{2p} or Q^{2i}) is not. The end-chain tetrahedra are noted Q^1. The tetrahedra linking two silicate chains in the interlayer space are noted Q^3 whereas the sites Q^2 next to Q^3 are named Q^{2v}. The calcium ions belonging to the main plane are noted Ca^{MP} whereas those in the interlayer are noted Ca^{IL}.

jennite with calcium of the main layer charge-balanced by OH^-, and a part of the protons of the SiOH are substituted by calcium ions.

Nonat and Lecoq proposed a slightly different model to account for the evolution of Ca/Si in the whole range from 0.66 to 2.[5] Contrary to Taylor's[6,17] and Cong and Kirpatrick's[7] models, it is not necessary to suppose a distorted structure. In the whole range of Ca/Si ratios, the XRD patterns of C-S-H samples always look like the tobermorite pattern, the *d* spacing corresponding to the basal plane only changes a bit; even at a high Ca/Si ratio close to 2, C-S-H samples do not look like jennite.[5] Then the main difference with the two previous models is the fact that there would not be a jennite-like region in the layers; that is, there would not be calcium of the main plane charge-balanced by OH^-. To reach significantly high Ca/Si values, Nonat and Lecoq's model supposes a charge balance of interlayered calcium by OH^-. Indeed, each missing bridging tetrahedron frees two crystallographic sites for oxygen of OH^- and allows the possibility to accommodate one $Ca(OH)_2$ unit in the structure. This model is as consistent with spectroscopic data as the previous ones even with those which demonstrate the presence of Ca−OH groups, since no model is precise enough until now to state that the Ca^{2+} ions belong to the main plane or to interlayer or both.

While there is no general agreement about the exact structural description of C-S-H, the evolution of stoichiometry with the chemical composition of the equilibrium solution is recognized. The chemical composition of the aqueous solution also greatly influences the structure of C-S-H, particularly the silicate chain's length. These structural modifications have been clearly evidenced in previous studies by solid-state NMR spectroscopy based mostly on ^{29}Si MAS NMR,[11,19−29] but also on ^{17}O NMR,[11,30,31] ^1H NMR[32,33] and even ^{43}Ca NMR.[34,35] In particular, ^{29}Si NMR spectroscopy[36] is very sensitive to the local organization of the various silicate species, and the chemical shift is the most informative parameter because it reflects the structural surroundings of a silicon atom. The silicate tetrahedra are usually named Q^n where Q represents the SiO_4 tetrahedron and *n* is the number of other tetrahedra to which it is linked. So Q^1 represents an end group of a chain, Q^2 a middle group, and Q^3 a branching site. Ranges of ^{29}Si chemical shifts of various silicate units have been determined,[36,37] but those shift ranges severely overlap so that a simple correlation of chemical shift and Q^n tetrahedra is not obvious and other information is required to fully assign all resonances in the ^{29}Si spectra and quantify their population after valuable deconvolutions. Unfortunately, despite numerous published data, only a few are quantitative because assignment of silicon sites is based on the simulations of the ^{29}Si NMR spectra.

Previous studies[16,35] have shown that it was possible to better characterize the structure of C-S-H through multinuclear NMR methodologies. Klur et al.[16] have employed $^{29}Si-^{29}Si$ correlation techniques to know whether silicon sites were in the same solid phase and also to clarify the neighboring between these silicon sites. Recently[38] new and deeper insights in the proton environment in C-S-H nanocrystals have been gained using a novel methodology for the analysis of the cross-polarization dynamics in NMR. This new strategy has proven to be a powerful tool for distinguishing two environments of protons by their different mobility, those in the internal interlayer space and those in the external surface of nanocrystalline C-S-H crystals.

The main aim of this contribution is to better characterize the local proton environment (hydroxyls, calcium ions or water molecules) of the silicate chains and also to gain information about the connectivity between silicate units in C-S-H within the Ca/Si range from 0.7 to 1.5. To better follow the structural evolution of the material, several NMR techniques have been applied. We performed two-dimensional $^1H-^{29}Si$ heteronuclear shift correlation experiments (HETCOR) at high spinning frequencies as well as double quantum homonuclear $^{29}Si-^{29}Si$ correlation experiments using the Back to Back recoupling scheme preceded by a cross-polarization $^1H-^{29}Si$ excitation. Complementary one-dimensional ^{29}Si CP/MAS spectra were recorded in order to reduce the measurement time and increase the sensitivity, as well as single pulse excitation (SPE) ^{29}Si spectra to obtain quantitative information about the distribution of various silicate sites and the average length of chains.

Experimental Section

Materials. ^{29}Si enriched (99.9%) SiO_2 was purchased from Isotec. C-S-H samples were prepared from mixture of CaO and enriched SiO_2 in stirred suspension with a H_2O to solid ratio of 50. The mixture was kept at 40 °C for 4 weeks. Samples were then filtered, washed by acetone and then ether and finally dried under low vacuum during 30 mn. Eight samples with Ca/Si ratio ranging from 0.7 to 1.5 were prepared.[33] Results presented here were obtained on enriched samples with Ca/Si ratios of 0.7

(cshe1), 0.9 (cshe3), and 1.5 (cshe7) and on a natural abundance sample with Ca/Si ratio of 1.45 prepared at 25 °C. All the samples show X-ray diffraction patterns characteristic of tobermorite like C-S-H (I) samples.[1]

NMR Methodologies. All NMR experiments were performed at room temperature on a Bruker Avance 500 spectrometer, operating at frequencies of 99.15 and 499.14 MHz for ^{29}Si and ^{1}H respectively, using a 4 mm o.d. Bruker CP-MAS probe. Single pulse excitation (SPE) ^{29}Si spectra were recorded at an MAS frequency of 15 kHz using a ^{29}Si 90° pulse length of 4 μs, a proton field decoupling of 40 kHz and a long recycle delay of 120 s necessary to yield quantitative spectra. It was also observed that, at such high spinning frequencies, the proton power decoupling has no effect on ^{29}Si line-widths. For ramped CP/MAS ^{29}Si and 2D ^{1}H−^{29}Si HETeronuclear chemical shift CORrelation (HETCOR), spectra were acquired using a MAS frequency of 15 kHz, a contact time of 1.8 ms and a recycle delay of 0.8 s. Proton spin lattice relaxation times (T_1) were measured by the inversion−recovery method and found to be shorter than 200 ms for the three enriched samples, which allow for very short recycle delays for cross-polarization (CP) experiments. The ^{1}H and ^{29}Si chemical shifts were referenced using tetrakis(trimethylsilyl)silane as the external reference. The ^{1}H NMR spectrum is characterized by one peak at 0.2 ppm and the ^{29}Si NMR spectrum by two peaks at −9.9 ppm and −135.3 ppm with respect to liquid tetramethylsilane.

Two-dimensional ^{1}H−^{29}Si HETCOR experiments were acquired under the same conditions. The ^{1}H 90° pulse (2.3 μs) was followed by a slightly ramped CP (10% power variation on the ^{1}H channel) to compensate the effects of experimental amplitude mismatch and to improve the transfer efficiency and the stability of these 2D experiments. 128 FIDs were acquired with rotor synchronized t1 increment of 66.6 μs.

Two-dimensional ^{29}Si−^{29}Si homonuclear double quantum correlation experiments were performed using the BAck to BAck (BABA) pulse sequence preceded by a cross-polarization ^{1}H−^{29}Si with a contact time of 1.8 ms for the three enriched samples. Other contact times in the range 1−4 ms were tested (data not shown) without significant difference. A slightly ramped CP (10% power variation on the ^{1}H channel) was also used. The spinning frequency was set to 10 kHz because lower recoupling efficiency was observed at higher spinning frequencies. The ^{29}Si 90° pulse was carefully calibrated using a two-dimensional nutation experiment directly on the sample. The dephasing time before the excitation period and after the reconversion period was set to 200 μs. 96 to 256 FIDs were acquired with 100 μs t1 increments.

Simulations. For each sample, the quantification of the silicon sites may be obtained from the fit of the SPE spectra or of the CPMAS spectra. On one hand, SPE spectra are quantitative but often suffer from low signal-to-noise ratio, even in enriched samples because of long ^{29}Si relaxation times. On the other hand, quantification from the (more sensitive) CPMAS spectra requires the knowledge of the parameters involved in the CP dynamics.[38] This can be rather a complex task. However, a great advantage of using the CPMAS data is the possibility of varying the intensity of each site by varying the contact time. Such a procedure often reveals the fine structure of the spectrum.[35] Thus, to use all the available data and to greatly improve the accuracy of our fit, we have developed a program which can fit several spectra simultaneously. This program uses the same spectral parameters (positions, line-widths and lines shapes) for all spectra but uses a varying intensity from one spectrum to another. Constraints can also be taken into account such as those provided by the homonuclear two-dimensional ^{29}Si spectra, especially the positions of the lines. Gaussian lines shapes were found to best fit our experimental data.

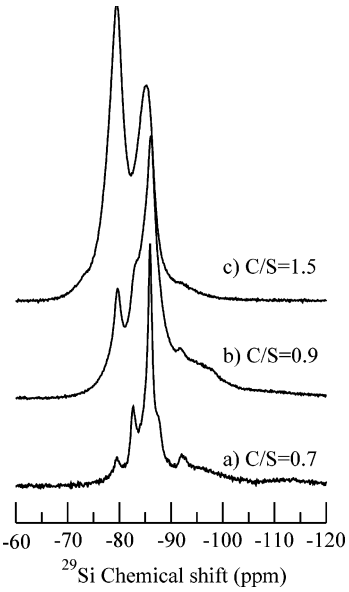

Figure 2. ^{29}Si MAS NMR spectra recorded by SPE at a spinning frequency of 15 kHz for three enriched C-S-H samples: (a) C/S = 0.7; (b) C/S = 0.9; (c) C/S = 1.5. 8k data points were acquired and zero filled to 16k points prior to Fourier transformation. No apodization was applied. The assignments of resonance lines are presented in Table 1 and discussed in the text.

Results and Discussion

^{29}Si MAS Spectra. Figure 2 shows SPE ^{29}Si high-resolution solid-state MAS NMR spectra of the three enriched C-S-H samples with Ca/Si ratios from 0.7 to 1.5. For the Ca/Si ratio of 0.7, a good resolution is observed with narrow resonance lines at −79.5, −82.6, −85.9 and −92 ppm. Two broad resonances at about −95 ppm and −110 ppm are also visible as already observed by Klur et al.[16] and attributed to Q^3 and Q^4 sites from residual silica used in the synthesis of C-S-H samples. The relative intensity of these broad signals decreases with the increasing Ca/Si ratio as expected. It is the less soluble part of the silica that remains in the sample. The shape of this part of the spectra depends not only on the amorphous silica used for the synthesis but also on the preparation conditions (hydration time, temperature, pH, drying, etc.). So the contribution of this residual silica signal is difficult to evaluate and interferes with the analysis of the ^{29}Si spectra. But as shown in Figure 3, the natural abundance C-S-H sample (Ca/Si = 1.45) presents a weaker contribution of the residual silica that simplifies the decomposition of the ^{29}Si MAS spectrum. This difference is attributed to the quality of the enriched silica used for the synthesis of C-S-H samples. Indeed the reactivity of the enriched silica is weaker due to the greater size of particles. No gain in resolution was obtained by using high power dipolar ^{1}H decoupling nor by increasing the MAS spinning frequency from 4 kHz to 15 kHz, meaning that the line-width must be due to chemical shift distribution rather than to dipolar couplings. Figure 2 shows that the resolution decreases with the increasing Ca/Si that may be due to either a weaker structural order or a larger distribution of chemical shifts associated with the chemical heterogeneity of the material resulting from the presence of residual silica or both. Indeed, the Ca/Si ratio of C-S-H close to silica may be locally lower than in the bulk of material.

TABLE 1: Chemical Shifts (ppm)[a] and Average Percentages[b] of ^{29}Si Sites for Different Calcium Silicate Hydrate Samples (Ca/Si = 0.7 to 1.5) from Simultaneous Simulations of ^{29}Si NMR Experimental Data (CP/MAS and SPE ^{29}Si NMR Spectra)

Q0	Q1	Q1	Q2p	Q2i	Q2-0	Q2-1	Q2v	Q3	Q3gel	Q4gel
					C/S = 0.7					
	−78	−79.6	−82.7	−84.6		−85.9	−87.7	−92.2	−93.4	−111
	<2%	4%	11%	7%		32%	4%	2%	27%	11%
					C/S = 0.9					
	−77.8	−79.6	−83	−84.7		−86.1	−88.3	−91.9	−96	
	4%	10%	14%	7%		39%	5%	3%	17%	
					C/S = 1.5					
−74.4	−77.4	−79.6	−82.2	−83.8	−85	−86			−91	
4%	7%	44%	4%	9%	10%	15%			7%	
					C/S = 1.45[c]					
	−77.5	−79.2	−81.5	−83.5	−85.1	−86.5	−89	−91.6	−99	
	<1%	46%	3%	6%	10%	3%	3%	2%	20%	

[a] The chemical shifts are given with ±0.1 ppm uncertainty. [b] The percentages are given with ±5% uncertainty. [c] Natural abundance sample.

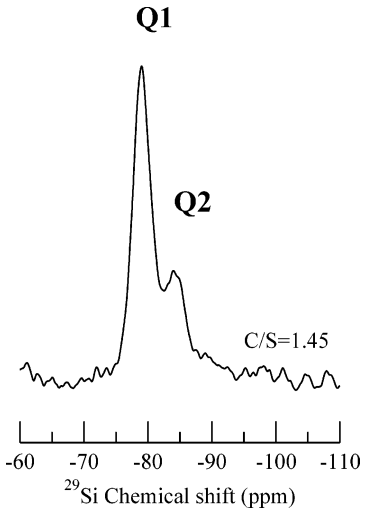

Figure 3. ^{29}Si MAS NMR spectrum recorded by SPE at a spinning frequency of 15 kHz for a natural sample at C/S = 1.45. 4k data points were acquired and zero filled to 8k points prior to Fourier transformation. The recycle time was 120 s and the number of scans was 288. Apodization of 10 Hz Lorentzian line broadening was used.

The main resonance lines observed at −79.5 ppm and at −85.9 ppm are due to end-chain tetrahedra Q^1 and nonbridging tetrahedra Q^2,[35,37] respectively. As the Ca/Si ratio increases, the intensities of these two resonances at −79.5 ppm and at −85.9 ppm increase and decrease, respectively. The increasing Q^1/Q^2 ratio indicates that the average chain length is decreasing in agreement with previous studies.[2,5,35] At Ca/Si = 0.7 a small intensity line at −82.6 ppm is attributed to the bridging tetrahedra Q^{2p} [16] with one hydroxyl and water molecules in the interlayer space. This assignment is further confirmed by the relative intensity of the Q^{2p}/Q^2 ratio found to be equal to the value 1/2. The fine peak at −92.5 ppm that appears in the Q^3 chemical shift range was assigned by Klur et al.[35] to Q^3 tetrahedra linking two silicate chains of two adjacent layers. This defect in comparison to the tobermorite structure was observed for the first time by Wieker et al.[39] and appears only at low Ca/Si ratios. A small shoulder at about −87.5 ppm is also visible (Figure 2) as previously observed.[35] This signal was assigned to Q^2 sites next to the Q^3 and named Q^{2v}. To better differentiate the signals, the spectra were acquired by cross-polarization with various contact times (from 50 μs to 18 ms). We observed different cross-polarization dynamics for the silicon sites[35,38] and in particularly at long contact times the signals of Q^{2v} and Q^3 sites are more intense. Nevertheless the resolution in these one-dimensional spectra is not sufficient to separate others lines. The advantage of two-dimensional correlation experiments is that the resolution of the 2D slices is much better due to two frequency dimensions compared to one-dimensional NMR spectra.

Double Quantum ^{29}Si−^{29}Si Experiments. There have been so far only few applications of ^{29}Si−^{29}Si homonuclear dipolar correlation techniques for the investigation of calcium silicate hydrate structure. Brough et al.[21] have recorded CPNOESY spectra with MAS at 2 kHz on enriched samples of C_3S hydrated at elevated temperatures. But due to long mixing times 2D spectra are not representative of dipolar ^{29}Si−^{29}Si connectivitites. Klur et al.[16] have used the sequences CPNOESY and BDR (broadband dipolar recoupling)[40] to identify the neighboring between the silicon sites and also to know if these sites belong or not to the same solid phase. However, using the sequence CPNOESY, the resolution is not sufficient to observe all the lines. The resolution is better with the BDR sequence, but certain silicon sites are unfortunately hidden by the intense diagonal peak.

Multiple-quantum (MQ) spectroscopy[41,42] is a very valuable tool for the structural characterization of spins systems. Homonuclear and heteronuclear high-resolution MQ experiments in solids with dipolar coupled spins and with fast MAS increase the resolution and the sensitivity. By means of double quantum experiments, the neighboring dipolar connectivities between like or different units Q^n units in disordered solids such as phosphates have been established by Feike et al.[43] The signals of DQ MAS spectra between like spins A resonating at the same chemical shift δ_A appears along the diagonal at (δ_A, $2\delta_A$), whereas the signals representing dipolar connectivities between nuclei with different chemical shifts δ_A and δ_B appear along the off-diagonal axis at (δ_A, $\delta_A+\delta_B$) and (δ_B, $\delta_A+\delta_B$). Larger intensities in off-diagonal peaks are generally due to a shorter distance between the dipolar coupled A−B nuclei. DQ spectroscopy may also be applied to probe phase separation in disordered materials. For the excitation of DQ coherences, the back-to-back (BABA) sequence has been used.[44] Another advantage of DQ MAS spectroscopy compared to the NOESY and BDR methods is that diagonal is informative.

The 2D ^{29}Si−^{29}Si homonuclear correlation spectra on the three enriched C-S-H samples with Ca/Si ratios of 0.7, 0.9 and 1.5 are presented in Figure 4. It can be observed that the resolution of 2D slices is better than those of simple one-dimensional spectra. The information gained in the 2D slices analysis is useful for further decomposition on spectra acquired by SPE that are sources of quantitative information.

For the sample at Ca/Si = 0.7, the 2D correlation spectrum (Figure 4a) corroborates the previous assignment of signals at

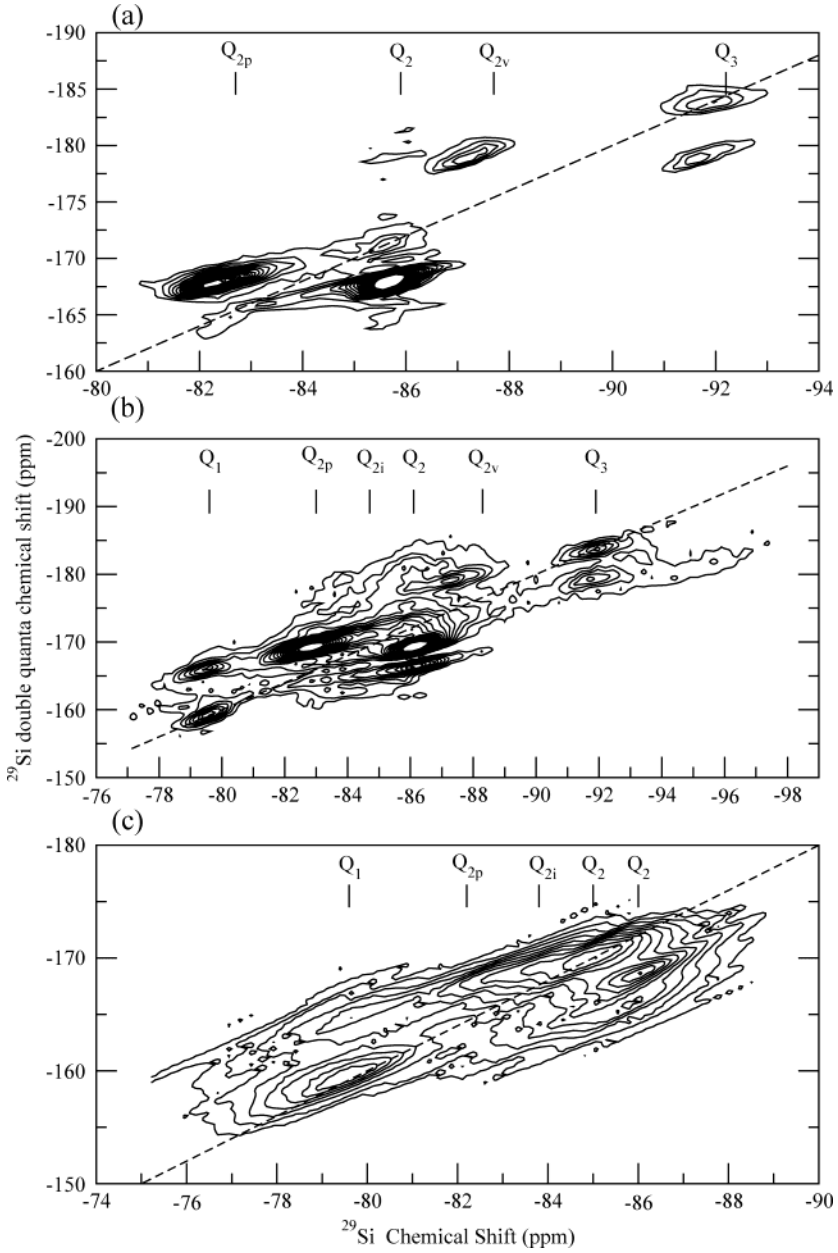

Figure 4. ^{29}Si double quantum homonuclear CP/MAS correlation NMR experiments recorded at a spinning frequency of 10 kHz on three enriched C-S-H samples: (a) C/S = 0.7; (b) C/S = 0.9; (c) C/S = 1.5. The double quantum coherences between identical spins appear along the diagonal, whereas the correlation peaks represent dipolar connectivities between silicon nuclei having different chemical shifts. 1536 to 6144 acquisitions were recorded for each of 96 to 256 t1 increments. The contact time was 1.8 ms for the three experiments using a 800 ms repetition delay. The 2D experiments were acquired in a States mode using a hypercomplex acquisition in order to obtain quadrature detection along F1. The 2D Fourier transforms were calculated using an echo-antiecho mode. No apodization was applied in F2 and F1 frequencies.

−79.5 ppm and at −85.9 ppm respectively to Q^1 and Q^2 tetrahedra, the Q^1 being either end-chain or dimer tetrahedra and the Q^2 being nonbridging tetrahedra. As no correlation between Q^1 is visible, it can be deduced that for this sample most of the Q^1 tetrahedra are end-chain Q^1. The correlation Q^1/Q^2 is not visible because it is too weak. The signal at −82.7 ppm is in the right border of the chemical shift range of Q^1 and in the middle of it for the Q^2. As it correlates with the Q^2 tetrahedra at −85.9 ppm it could be assigned to bridging Q^2 silicon thereafter noted Q^{2p}. This is in agreement with previous assignments.[16] The resonance at −92 ppm is in the Q^3 chemical shift range but also in the border of the Q^2 shift range. Klur[35] assigned it to Q^3 linking two silicate plans. As visible in Figure 4, its intensity decreases with increasing Ca/Si ratio. From the fact that the probability of having interconnection between silicates plan decreases with Ca/Si ratio increasing, we can assign it to Q^3 tetrahedra. The signal at −87.5 ppm is in the chemical shift range of Q^2 silicate only and is correlated with the Q^3 signal, so we can assign it to Q^2 tetrahedra of the chain linked with Q^3 silicon and note it Q^{2v}.[16] This signal that is only seen as a shoulder on the MAS and CP/MAS spectra is clearly shown in the 2D correlation spectrum although the expected correlation between Q^2 and Q^{2v} resonances is not clearly visible. On the diagonal, correlations Q^2/Q^2 and Q^3/Q^3 are clearly visible. So far our assignments are in agreement with those of Klur et al.[16] There are also indications of other signals between the Q^{2p} and Q^2 resonances, but due to the lack of resolution no further indication on the local environment of silicate chains can been obtained. Differences in intensities of the off-diagonal peaks cannot be directly related to variations in distances between the silicon sites, as cross-polarization was used in these experiments.

On the 2D correlation spectrum (Figure 4b) of the Ca/Si = 0.9 sample, stronger correlation peaks are visible for the Q^1 tetrahedra. Q^1-Q^1 correlation peaks are observed. This could be explained in two ways: whether they are end-chain Q^1 that correlate with Q^1 of another chain, or whether they are dimeric Q^1. In tobermorite, the distance between two Q^2 neighbors is 3.1 Å, giving a $^{29}Si-^{29}Si$ dipolar coupling of 160 Hz; the distance between two Q^1 of a dimer should be very close to that value. In the same way, the distance between two Q^1 of a neighboring chain must be close to the distance separating two Q^2 linked by a Q^{2p}. In tobermorite this distance is 4.3 Å, giving a dipolar coupling of 60 Hz. So, correlation between dimeric Q^1 must be a lot more effective than between Q^1 of adjacent chains; therefore, the Q^1/Q^1 correlations we observe can be attributed to the dimer. We observe also correlations between Q^{2p} (−82.9 ppm) and Q^2 (−86.1 ppm) and much less intense correlations between Q^{2v} (−87.3 ppm) and Q^3 (−91.9 ppm). Other weak correlations not yet assigned are also visible. There are also correlations between Q^1 and Q^2, the cross-peaks being much more intense than for the first sample (Ca/Si = 0.7). This denotes shortening of the silicate chain while the Ca/Si ratio is increasing. It is not the average chain length, as we can discriminate between dimer Q^1 and end chain Q^1. These double quantum $^{29}Si-^{29}Si$ experiments allow simultaneous observation of the formations of Q^1 dimers and the decrease of the chain length for the increasing Ca/Si ratio. This differs with previous results of Cong and Kirkpatrick[45] who postulated a bimodal distribution of chain length. Their CP/MAS ^{29}Si NMR data showed that Q^1 and Q^2 silicon see proton reservoirs with different $T_{1\rho}{}^1H$ values, indicating the presence of dimers and relatively long chains. They concluded that the increasing Ca/Si ratio leads to the formation of dimers but that the chain length remains constant. Yet the experimental data of cross-polarization was analyzed assuming a fast CP regime ($T_{IS} < T_{1\rho}$) when it is the reverse situation (i.e. $T_{IS} > T_{1\rho}$), slow regime) that occurs in CSH, as recently demonstrated.[38] To distinguish between the two situations and to take into account this unusual situation ($T_{IS} > T_{1\rho}$), the Torque experiment was used.[46] Thus, it was possible to differentiate two environments of protons by their different relaxation rates and interpret as being the internal interlayer space and the external surface of C-S-H crystals. These 2D experiments demonstrated the continuous decrease of the silicate chains and the formation of dimers at high Ca/Si ratios.

On the third 2D correlation spectrum (Figure 4c) of the Ca/Si = 1.5 sample, the lines are larger, resulting in a low resolution, probably due to a more important structural disorder in the material. The sites Q^{2v} and Q^3 have disappeared. Only correlations Q^1/Q^1, Q^1/Q^2 and Q^2/Q^2 are clearly observed as indicated on the Figure 4c. In the asymmetry of the Q^2/Q^2 correlation appear some Q^{2p}/Q^2 and Q^{2i}/Q^2 correlations; the Q^{2i} tetrahedra are bridging tetrahedra with hydroxyl, water and a calcium ion neighbor. There are hence two Q^2 sites, at respectively −86 ppm and −85 ppm. There is also some fine structure in the Q^1/Q^1 area, but further conclusions would be difficult at this step due to broader resonance lines at this high Ca/Si ratio. Though a better separation of resonance lines would allow more refined structural information to be obtained, the local evolution of the silicate chains with increasing Ca/Si ratio is clearly shown.

$^1H-^{29}Si$ Correlation Experiments. Protons play an important role in the calcium silicate hydrate, as they contribute, for instance, to the cohesion between the layers through hydrogen bonds. Nevertheless, the different proton species (water molecules, CaOH and SiOH environments, etc.) are difficult to identify on the ^1H NMR spectrum as a result of its low resolution: chemical shift range is small and lines are broad, typically 2500 Hz. Dipolar homonuclear $^1H-^1H$ interactions and chemical shifts distributions are responsible for this broadness. High-speed (up to 16 kHz) ^1H MAS NMR experiments performed by Heidemann[32,47] on polycrystalline silicates allowed characterization of the nature of protons by their chemical shifts, and a ^1H chemical shift range on poorly crystalline calcium silicate hydrate could be established. The isotropic ^1H chemical shifts of the protons in the H_2O molecules are in a small range between +6 ppm and +3 ppm,[32,47] whereas the ^1H chemical shifts in CaOH groups resonate in a range between +4 ppm and −2 ppm. For protons in SiOH groups of silicates, the relatively large range extends between +15 ppm and +6 ppm.[32,47] Such high ^1H NMR chemical shifts have been observed in a few silicates[48,49] and arise from strongly hydrogen-bonded protons involving SiOH groups. From the linear relationship of Eckart and co-workers[50] between chemical shift and bond length, high ^1H NMR chemical shifts correspond to short −O−H···O− distances and are consistent with strong hydrogen bonding of hydroxyl groups.

In our investigations we have used the 2D HETCOR NMR techniques described in the literature[51] which is one of the most important methods to elucidate the molecular structure by correlating the chemical shifts of different nuclei through space dipolar interactions. In the 2D HETCOR NMR experiment, only correlations between spatially nearby species can be observed because the dipolar couplings vary inversely with the cube of the distance between the spins. Motion can also reduce the magnitude of dipolar couplings and hence the distances over which correlations are observed. The aim is to observe only protons which contribute to the C-S-H structure and to exclude protons in pores. In this experiment only protons at short distances (about 5 Å) from the silicon sites can be observed via an efficient magnetization transfer. It may also indicate that the observed protons belong to the same phase as the C-S-H crystallites. Another advantage of the 2D experiments is the better resolution of spectra due to two frequency dimensions, compared to 1D NMR, which yields easier the decomposition of spectra. In our 2D $^1H-^{29}Si$ experiments acquired under fast MAS at 15 kHz no heteronuclear decoupling was used because no improvement of the resolution was observed using ^1H broadband decoupling. Homonuclear $^1H-^1H$ couplings were eliminated by the high speed so that no $^1H-^1H$ decoupling was needed during the evolution period. The advantage is that there is no scaling factor in the dimension F1 like for instance in the sequence BLEW-12.[52]

The 2D $^1H-^{29}Si$ heteronuclear correlation spectra acquired with the HETCOR sequence on the three enriched C-S-H samples with Ca/Si ratios of 0.7, 0.9 and 1.5 are presented in Figure 5 along with one-dimensional projections along each axis. The relative intensities of signals are not quantitative, as they depend on the efficiency of cross-polarization. As shown in Figure 5, the signal-to-noise ratio in HETCOR spectra decreases with the Ca/Si ratio. It is more related to experimental parameters of cross-polarization, to the strength of the heteronuclear dipolar interactions, and also to the relaxation times in the rotating frame $T_{1\rho}$ of protons,[38] than to the hydration levels in the samples that are expected to decrease with the Ca/Si ratio. The 2D $^1H-^{29}Si$ HETCOR experiments indicate the presence of several cross-peaks between silicon and proton species. At Ca/Si = 0.7 (Figure 5a), the correlation map clearly shows four peaks Q^1, Q^{2p}, Q^2 and Q^3 peaks at respectively −79.5 ppm,

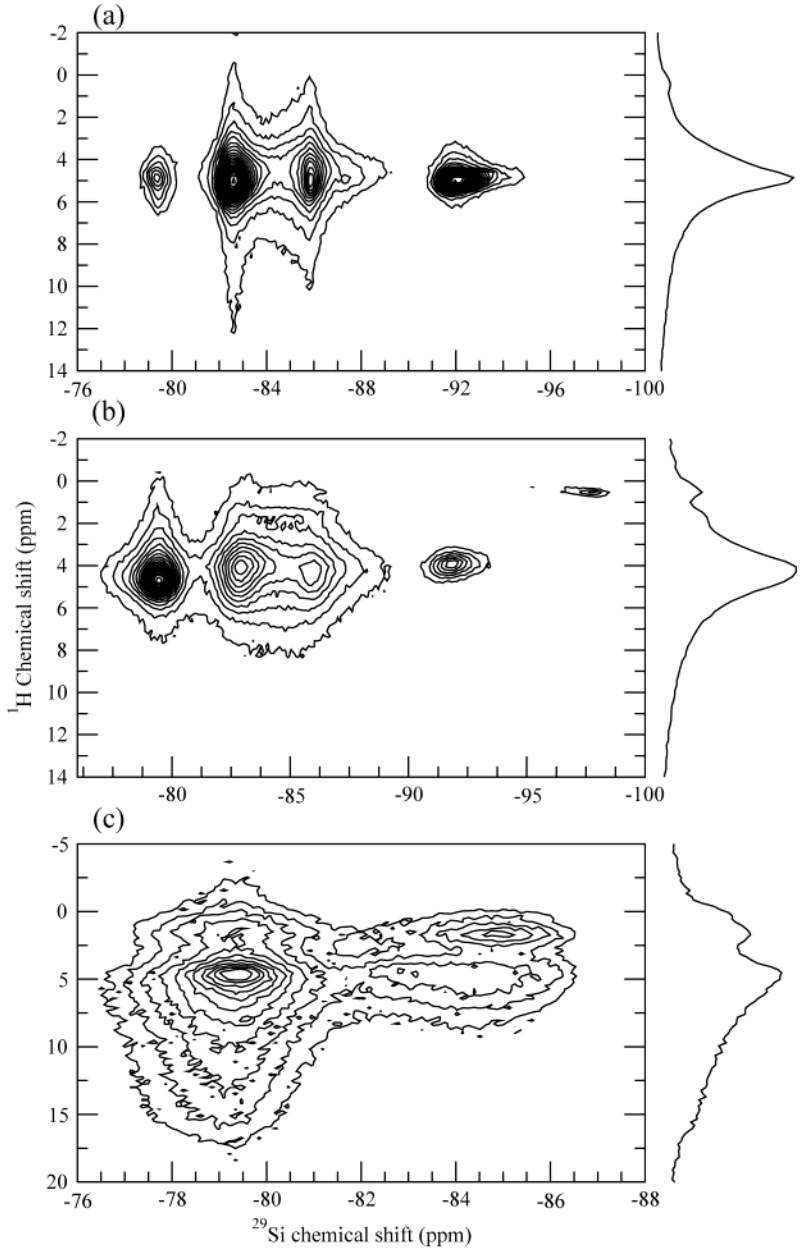

Figure 5. 2D ^{29}Si−^{1}H heteronuclear chemical shift correlation (HETCOR) NMR experiments recorded at 15 kHz on three enriched C-S-H samples: (a) C/S = 0.7; (b) C/S = 0.9; (c) C/S = 1.5. 544 acquisitions were recorded for each of the 128 t1 increments using a 800 ms repetition delay. The contact time was set to 1.8 ms. The ^{1}H MAS projection is shown along the vertical axis. The 2D experiments were acquired in a States mode for quadrature detection in F1. The 2D Fourier transforms were calculated using an echo-antiecho mode. No apodization was applied for F2 and F1 frequencies.

−82.7 ppm, −85.8 ppm and −92 ppm. The site Q^{2v} corresponding to Q^2 next to Q^3 is also visible at −87.7 ppm from the ^{29}Si projection spectrum. The ^{1}H projection spectrum consists of a main resonance at 4.9 ppm ($\Delta\upsilon_{1/2}$ = 100 Hz). All the silicon sites are polarized by the same ^{1}H signal at 4.9 ppm. This resonance can be attributed to water molecules and perhaps also Si−OH groups in exchange. Indeed the 2D ^{1}H slices indicate that protons which polarize Q^3 have fine lines (about 600 Hz), whereas the Q^{2p} and Q^2 are polarized by protons whose lines are larger (1000 to 1300 Hz) perhaps due to the exchange H_2O/SiOH. It means that in this CSH sample, the water molecules are the main source of cross-polarization for all the silicon sites in the interlayer space. Our observations are in agreement with previous observations[16] but here higher resolution enables to observe differences between sites from ^{1}H and ^{29}Si slices.

For the other C-S-H sample (Ca/Si = 0.9) (Figure 5b), the ^{29}Si projection spectrum shows that the site Q^{2v} is no more visible whereas a new site at −84.6 ppm can be observed and attributed to Q^{2i}. The ^{1}H projection spectrum shows a main resonance at 4.7 ppm with a moderate broadening attributed to H_2O protons and also a small signal at 1.9 ppm which could arise from basic groups such as CaOH protons according to literature data.[32,47] We observe also a broad shoulder which extends between about 7 and 12 ppm and which could correspond from the chemical shift range[32,47−49] to protons in SiOH groups. No individual lines are visible, but signals at higher chemical shifts could be due to hydrogen-bonded SiOH as it was previously observed in polysilicates.[48,49] The analysis of 2D ^{1}H slices shows that the silicon sites are in different protons environments: the protons which polarize Q^3 have narrow lines (about 600 Hz) and resonate at 4.1 ppm (H_2O

TABLE 2: Variations of Q^{2pS}/Q^{2npS} and Q^1/Q^2 with the Ca/Si Ratio for Different Calcium Silicate Hydrate Samples[a,b]

C/S	Q2pS/Q2npS	Q1/Q2
0.7	0.5	0.1
0.9	0.48	0.2
1.5	0.52	1.3
1.45[c]	0.56	2

[a] $Q^{2pS} = Q^{2p} + Q^{2i}$. [b] $Q^{2npS} = Q^{2-0} + Q^{2-1} + Q^{2v}$. [c] Natural abundance sample.

protons) whereas the Q^{2p}, Q^{2i} and Q^2 are polarized by protons whose lines resonate at about 4.3 ppm and are larger (1300 to 1900 Hz). Moreover, the sites Q^{2i} and Q^2 are also polarized by CaOH protons which resonate at 1.9 ppm. The Q^1 are polarized only by protons at 4.7 ppm probably arising from H_2O and SiOH protons.

Finally, at high Ca/Si ratio (1.5) (Figure 5c), the ^{29}Si resonances lines as well as ^1H lines are broader probably due to a distribution of chemical shifts in a more disordered environment. In the ^1H dimension, three different protons species are clearly observed: first, H_2O protons at about 4.6 ppm correlated with Q^1, Q^{2p} and Q^2 sites, CaOH protons at 1.8 ppm correlated with all silicon species, and a broad resonance between 7 and 17 ppm corresponding to Si−OH protons correlated also with all silicon species. Here we only observe a large distribution of chemical shifts, but such high ^1H NMR chemical shifts can be attributed to silanol protons with hydrogen bonding, as reported in the literature.[32,47−49] The gain in resolution compared to MAS and CP/MAS 1D spectra is useful, as the Q^{2p} resonance at −82.9 ppm is visible on the 2D experiment, whereas it only appears as a shoulder in one-dimensional spectra. The presence of these bridging tetrahedra indicates that the "dreierketten" chain structure is still conserved at this Ca/Si ratio of 1.5. Although the lines intensities in the ^1H projections are not quantitative, the influence of the increase of the Ca/Si ratio is clearly to raise the amount of calcium ions that are in the interlayer space. In these experiments, being recorded in the same conditions, the increase can be roughly followed by monitoring the rise of CaOH proton's signal in the ^1H projection.

A rather surprising observation is the higher intensity observed for Si−OH protons at Ca/Si = 1.5 rather than at low Ca/Si ratio as expected. This result could be explained by the molecular motion and exchange between protons which would significantly reduce the heteronuclear dipolar coupling and thus the efficiency of cross-polarization. This exchange process would be more efficient at low Ca/Si ratios. Previous observations[45] have shown that the cross-polarization of silicon sites in some C-S-H samples is more efficient at low temperatures due to the reduction of the proton motions, and it could be informative to perform these 2D HETCOR experiments at variable temperature to get some insight on the exchange between the protons.

Structural Model. In the case of our samples, structural and quantitative information respectively deduced from 2D $^{29}Si-^{29}Si$ homonuclear correlation experiments and 1D ^{29}Si SPE spectra, indicate that the ratio of bridging to nonbridging Q^2 sites remains close to 0.5 (Table 2) whatever the Ca/Si ratio is, meaning that the "dreierketten" structure is retained even at high Ca/Si ratio (1.5). The shortening of the silicate chains with the increasing Ca/Si ratio is clearly demonstrated by the Q^1/Q^2 ratio (Table 2). At Ca/Si = 0.7 the ratio Q^1/Q^2 equal to 0.1 corresponds to a chain length of about 20 silicate tetrahedra, i.e., about 70 Å. At Ca/Si = 0.9, the chain length decreases as indicated by the ratio Q^1/Q^2 equal to 0.2, but the modification is the most striking at high Ca/Si ratio (1.5): the percentage of Q^1 sites has strongly increased and the Q^1/Q^2 equal to 1.3 shows that the chain length has largely decreased. For the natural abundance sample (Ca/Si = 1.45), this ratio is still higher; it is probably due to the fact that it was synthesized at a lower temperature. Indeed, it is generally observed that for a given Ca/Si ratio, the chain length increases with temperature. Our results are in good agreement with other data based on ^{29}Si NMR experiments[7,16] showing that the silicate chain length decreases as the Ca/Si increases from 0.7 to about 1.5. The decreasing polymerization of our samples with increasing Ca/Si follows the predicted linear correlation between Ca/Si ratio and $Q^1/Q^1 + Q^2$ ratio calculated according to the tobermorite model proposed by Cong and Kirkpatrick.[7] As shown in Figure 4, a more important disorder is visible for this material at Ca/Si = 1.5. It was equally observed by infrared spectroscopy[53] on C-S-H samples at Ca/Si ratio equal to about 1.3. These observations are not in favor of the jennite structure where the silicate chains are more ordered.

CaOH environments were observed in various C-S-H samples using different spectroscopic methods.[12,16,54] Ca-EXAFS experiments in C-S-H[12] have shown that the calcium environment does not depend on the Ca/Si ratio (from 0.7 to 1.4) and that this environment is similar to that observed in tobermorite. Very recently Thomas et al.[54] measured by inelastic neutron spectroscopy the content of CaOH bonds in hydrated tricalcium silicate ($3CaO{\cdot}SiO_2$) and white Portland cement pastes and suggested that the structure of C-S-H gel at Ca/Si = 1.7 looks like jennite more closely than that of tobermorite. This suggestion is based upon the hypothesis that the Ca−OH bonds occur in the main Ca−O sheet. However, the CaOH environments could be located in the interlayer or on surface sites taking into account the high surface volume ratio.

2D $^1H-^{29}Si$ HETCOR experiments clearly showed in our samples the presence of Ca−OH protons at higher Ca/Si ratio. Since $^1H-^{29}Si$ cross-polarization experiments are used, only protons next to silicon atoms can be detected. So Ca−OH protons observed on the ^1H projection spectrum correspond to Ca−OH protons inside the C-S-H structure. At Ca/Si = 0.9, these protons are correlated with Q^{2i} silicon sites, suggesting that they are in the interlayer space together with Ca ions. At Ca/Si = 1.5, Ca−OH protons are correlated with all silicon sites, the Q^{2i} closer to the calcium ions in the interlayer space (Ca^{IL}, Figure 1), and Q^1 and Q^2 silicon sites closer to the calcium of the main plane (Ca^{MP}, Figure 1). It is then possible to consider two hypotheses to account for this evolution: first, due to the decrease of the interlayer space associated with the increase of Ca/Si ratio,[24] interlayer Ca−OH are close enough to all silicon sites to be correlated with them. In the second hypothesis, one can consider that part of the Ca ions of the main plane are coordinated by oxygen of OH^- in place of silicate; thus, there would be calcium hydroxide type or/and jennite type areas in the structure according to the model proposed by Cong and Kirkpatrick,[7] but it probably changes more in the X-ray diffraction pattern that is observed so the authors believe the first hypothesis is more probable. In this case, according to the defect tobermorite model and following the distribution of the different sites given Table 1, about half of the silicate chains are dimers corresponding to the average formula for the part of main layer $Ca_2H_2Si_2O_7$ if all the bending bonds are protonated. The other half is pentamers corresponding to the average formula for the part of main layer $Ca_4H_4Si_5O_{16}$ if all the bending bonds are also protonated. With this last hypothesis, the Ca/Si

ratio should be only 0.85. On the other hand, if all the protons are substituted by calcium ions at the internal surface sites, according to the following equilibrium in the interlayer:

$$2\ \mathrm{Si{-}OH} + \mathrm{Ca^{2+}} \rightarrow \mathrm{SiO{-}Ca{-}OSi} + 2\mathrm{H^{+}}$$

the Ca/Si ratio is only 1.28. To reach a Ca/Si ratio close to 1.5, the following substitution has to be considered for all the silanol groups at the external and internal surface sites:

$$\mathrm{Si{-}OH} + \mathrm{Ca^{2+}} + \mathrm{OH^{-}} \rightarrow \mathrm{SiO{-}Ca{-}OH} + \mathrm{H^{+}}$$

In fact, 2D HETCOR experiments show that SiOH groups are always remaining in the structure so a non-negligible part of the Ca^{2+} ions associated with 2 OH^{-} groups to ensure the charge balance is present in the C-S-H phase at high Ca/Si ratio.

Conclusion

This work has shown the power of double quantum homonuclear 2D $^{29}Si{-}^{29}Si$ correlation spectroscopy combined with a cross-polarization excitation to obtain information about the connectivity between silicate chains in ^{29}Si-enriched C-S-H samples. The dipolar connectivities can be established and the structural evolution with the ratio Ca/Si is clearly demonstrated by the continuous decrease of the silicate chain length and the formation of Q^1/Q^1 dimers. The 2D $^{1}H{-}^{29}Si$ heteronuclear chemical shift correlation spectra using fast magic-angle sample spinning have allowed better characterization of the proton environnment. At low Ca/Si ratio, the water molecules are the main source of cross-polarization for all the silicon sites in the interlayer space probably because of its proximity to the silicon atoms. At high Ca/Si ratio, the presence of Ca−OH protons in the interlayer space is clearly visible. These protons are correlated to all the silicon species. From a structural point of view, these results have shown that the C-S-H structure stays close to the tobermorite one and that the "dreierketten" unit is retained even at high Ca/Si ratio. For the 2D HETCOR spectra, a more efficient cross-polarization could be probably obtained by working at lower temperature to decrease the molecular motion. This work also shows the possibility to use heteronuclear correlation experiments with samples made with ^{29}Si natural abundance samples. It should be possible now to investigate further fully hydrated tricalcium silicate pastes which may be believed more representative of C-S-H in cement pastes.

References and Notes

(1) Taylor, H. F. W. *Cement Chemistry*; Academic Press: London, 1990.
(2) Grutzeck, M.; Benesi, A.; Fanning, B. *J. Am. Ceram. Soc*. **1989**, *72*, 665.
(3) Taylor, H. F. W. *J. Chem. Soc*. **1950**, *72*, 3682.
(4) Damidot, D.; Nonat, A.; Barret, P.; Bertrandie, D.; Zanni, H.; Rasem, R. *Adv. Cem. Res.* **1995**, *7*, 1.
(5) Nonat, A.; Lecoq, X. *NMR Spectroscopy of Cement Based Materials*; Springer: Berlin, 1998; p 197.
(6) Taylor, H. F. W. *J. Am. Ceram. Soc.* **1986**, *69*, 464.
(7) Cong, X.; Kirpatrick, R. J. *Adv. Cem. Based Mater*. **1996**, *3*, 144.
(8) Gauffinet, S.; Finot, E.; Lesniewska, E.; Nonat, A. *C. R. Acad. Sci. Paris* **1998**, *327*, 231.
(9) Lognot, I.; Klur, I.; Nonat, A. *NMR Spectrocopy of Cement Based Materials*; Springer: Berlin, 1998; p 189.
(10) Yu, P.; Kirpatrick, R. J.; Poe, B.; McMillan, P. F.; Cong, X. *J. Am. Ceram. Soc*. **1999**, *82*, 742.
(11) Cong, X.; Kirpatrick, R. J.; Yarger, J. L.; McMillan, P. F. *NMR Spectrocopy of Cement Based Materials*; Springer: Berlin, 1998; p 143.
(12) Lequeux, N.; Morau, A.; Philippot, S.; Boch, P. *J. Am. Ceram. Soc.* **1999**, *82*, 1299.
(13) Kirpatrick, R. J.; Brown, G. E.; Xu, N.; Cong, X. *Adv. Cem. Res*. **1997**, *9*, 31.
(14) Hamid, S. A. *Zeitschrift fûr Kristallographie* **1981**, *154*, 189.
(15) Minard, H. *Thesis*, Dijon, France, 1999.
(16) Klur, I.; Pollet, B.; Virlet, J.; Nonat, A. *NMR Spectrocopy of Cement Based Materials*; Springer: Berlin, 1998; p 119.
(17) Carpenter, A. B. C.; Gard, J. A.; Speakman, K.; Taylor, H. F. W. *Am. Mineral.* **1966**, *51*, 56.
(18) Taylor, H. F. W. *Adv. Cem. Based Mater*. **1993**, 38.
(19) Clayden, N.; Dobson, C.; Hayes, C.; Rodger, S. J. *J. Chem. Soc. Chem Commun.* **1984**, 1396.
(20) Brough, A.; Dobson, C. *J. Am. Ceram. Soc*. **1994**, *77*, 593.
(21) Brough, A. R.; Dobson, C. M.; Richardson, I. G.; Groves, G. W. *J. Mater. Sci*. **1994**, *29*, 3926.
(22) Grimmer, A. *Application of NMR spectroscopy to cement science*; Gordon and Breach, Amsterdam, 1993; p 113.
(23) Lippmaa, E.; Mägi, M.; Tarmak, M.; Wieker, W.; Grimmer, A. R. *Cem. Concr. Res.* **1982**, *12*, 1282.
(24) Bell, G.; Benstedt, J.; Glasser, F.; Lachowski, E.; Roberts, D.; Taylor, M. *Adv. Cem. Res.* **1990**, *3*, 23.
(25) Masse, S.; Zanni, H.; Lecourtier, J.; Roussel, J.; Rivereau, A. *J. Chim. Phys*. **1995**, *91*, 4423.
(26) Bresson, B.; Masse, S.; Zanni, H.; Noik, C. *NMR Spectrocopy of Cement Based Materials*; Springer: Berlin, 1998; p 209.
(27) Hjorth, J.; Skibsted, J.; Jakobsen, H. *Cem. Concr. Res*. **1988**, *18*, 789.
(28) Young, J. *J. Am. Ceram Soc*. **1994**, *77*, 765.
(29) Noma, H.; Adachi, H.; Yamada, T.; Nishino, Y.; Matsuda, Y.; Yokoyama, T. *NMR Spectrocopy of Cement Based Materials*; Springer: Berlin, 1998; p 159.
(30) Cong, X.; Kirpatrick, R. J. *Cem. Concr. Res*. **1993**, *23*, 1065.
(31) Cong, X.; Kirpatrick, R. J. *J. Am. Ceram. Soc*. **1996**, *79*, 1585.
(32) Heidemann, D.; Wieker, W. *NMR Spectrocopy of Cement Based Materials*; Springer: Berlin, 1998; p 169.
(33) Rassem, R.; Zanni, H.; Heidemann, D.; Grimmer, A. R. *Cem. Concr. Res*. **1993**, *23*, 169.
(34) Nieto, P.; Dron, R.; Thouvenot, R.; Zanni, H.; Brivot, F. *C. R. Acad. Sci. Paris* **1995**, t320, Serie II, 485.
(35) Klur, I. *Thesis*, Paris VI, 1996.
(36) Engelhardt, G.; Michel, D. *High-resolution solid-state NMR of silicates and zeolites*; Wiley: Chichester, 1987, Chapter 4.
(37) Lippmaa, E.; Mägi, M.; Samoson, A.; Engelhardt, G.; Grimmer, A. R. *J. Am. Chem. Soc*. **1980**, *102*, 4889.
(38) Klur, I.; Jacquinot, J.-F.; Brunet, F.; Charpentier, Th.; Virlet, J.; Schneider, C.; Tekely, P. *J. Phys. Chem. B* **2000**, *104*, 10162.
(39) Wieker, W.; Grimmer, A. R.; Winkler, A.; Mägi, M.; Tarnak, M.; Lippmaa, E. *Cem. Concr. Res*. **1982**, *12*, 333.
(40) Sodickson, D. K.; Levitt, M.; Vega, S.; Griffin, R. G. *J. Chem. Phys*. **1993**, *98*, 6742.
(41) Ernst, R. R; Bodenhausen, G.; Wokaun, A. *Principles of Nuclear Magnetic Resonance in One and Two Dimensions*; Clarendon Press: Oxford, 1987.
(42) Schmidt-Rohr, K.; Spiess, H. W. *Multidimensional Solid State NMR and polymers*. Academic Press: New York, 1994.
(43) Feike, M.; Demco, D. E.; Graf, R.; Gottwald, J; Hafner, S.; Spiess, H. W. *J. Magn. Reson. A* **1996**, *122*, 214.
(44) Demco, D. E.; Hafner, S.; Spiess, H. W. *J. Magn. Reson. A* **1995**, *116*, 36.
(45) Cong, X.; Kirpatrick, R. J. *Adv. Cem. Res*. **1995**, *7*, 103.
(46) Tekely, P.; Gérardy, V.; Palmas, P.; Canet, D.; Retournard, A. *Solid State NMR*, **1995**, *4*, 361.
(47) Heidemann, D. *Application of NMR spectroscopy to cement science*; Gordon and Breach, Amsterdam, 1993; p77.
(48) Almond, G. G.; Harris, R. K.; Graham, P.; *J. Chem. Soc.; Chem. Commun*. **1994**, 851.
(49) Gardiennet, C.; Tekely, P. *J. Phys. Chem. B* **2002**, *106*, 8928.
(50) Eckart, H.; Yesinowski, J. P.; Silver, L. A.; Stolper, E. M. *J. Phys. Chem*. **1988**, *92*, 2055.
(51) Vega, A. J. *J. Am. Chem. Soc*. **1988**, *110*, 1049.
(52) Burum, D. P.; Linder, M.; Ernst, R. R. *J. Magn. Reson*. **1981**, *44*, 173.
(53) Yu, P.; Kirkpatrick, R. J.; Poe, B.; Mc Millan, P. F.; Cong, X. *J. Am. Ceram. Soc*. **1999**, *82*, 742.
(54) Thomas, J. J.; Chen, J. J.; Jennings, M. *Chem. Mater*. **2003**, *15*, 3813.